Enhanced high-order harmonic generation via controlling ionization in spatially extended systems

Qingbin Zhang,[1] Peixiang Lu,[1,2,*] Weiyi Hong,[1] Qing Liao,[1] Pengfei Lan,[1] and Xinbing Wang[1]
[1]*Wuhan National Laboratory for Optoelectronics, Huazhong University of Science and Technology, Wuhan 430074, People's Republic of China*
[2]*State Key Laboratory of Precision Spectroscopy, East China Normal University, Shanghai 200062, People's Republic of China*
(Received 11 December 2008; revised manuscript received 17 March 2009; published 8 May 2009)

We theoretically investigate the high-order harmonic generation when the spatially extended systems are irradiated by a two-color laser field. By controlling electron ionization, the $\omega+2\omega$ excitation scheme creates efficient harmonics radiation beyond $I_p+3.17U_p$ with both odd and even harmonics. Calculations show that the harmonics beyond $I_p+3.17U_p$ are well phase locked, moreover, the chirp rate is only 3 as/eV. Using a 5 fs driving pulse, the bandwidth supporting isolated attosecond pulse in harmonic spectrum is 125 eV, and a 68 as single pulse can be obtained straightforwardly.

DOI: 10.1103/PhysRevA.79.053406 PACS number(s): 33.80.Wz, 42.65.Ky, 42.65.Re

I. INTRODUCTION

High-order harmonic generation (HHG) is an interesting subject for its potential as table-top source of coherent ultrafast extreme-ultraviolet (xuv) radiation up to water window spectral range. The process of HHG was first studied in atoms and has been well understood in terms of semiclassical three-step model [1]. An electron is ejected in the continuum after tunneling through the atomic potential barrier formed by the instantaneous laser field. Subsequently, the electron oscillates almost freely in the laser field and gains kinetic energy E_k. The electron may revisit the parent ion at each half of laser period to recombine and emit a burst of continuum extreme-ultraviolet radiation. A typical harmonic spectrum presents a broad plateau and a sharp cutoff; these attractive properties indicate that HHG is a strong candidate for obtaining xuv attosecond pulses. Continuing efforts have been paid to produce attosecond pulse trains [2–4] and isolated pulses [5–9] from harmonic spectrum.

The HHG spectrum itself is also a sensitive detector of attosecond processes in the atomic and molecular nonlinear medium [10,11]. Some recent experiments have discussed this issue using HHG from molecules and found some novel phenomena that relate directly back to the electron evolution in molecule and molecular structure [12,13]. However, compared to the study of high harmonic and attosecond pulse generation from atoms, fewer efforts have been devoted to the more complicated systems such as atomic cluster and molecule. It was found that atoms and small molecules behave similarly as far as the broad features of HHG [14,15] because the wavepacket associated to the recollding electron is typically much lager than the internuclear distance. For example, the harmonic spectra contain a nonperturbative plateau with a cutoff at a photon energy which is about $I_p+3.17U_p$ in both cases, where U_p is the ponderomotive energy and I_p is the ionization potential. However, since molecules have more degrees of freedom than atoms, their behaviors in strong fields are richer [10,11,13,16,17]. The two-center structure of molecule allows us to generate higher-order harmonics: the electron may be detached from one nucleus then be accelerated by the laser field toward another nucleus, where it is captured and emits an energetic photon. In stretched molecules, the harmonic spectrum can be extended to I_p+8U_p at specific internuclear distance [17]. In comparison to experiments performed in atoms, HHG from atomic clusters has also shown enhancement of the harmonic cutoff [18,19]. Recently, it was demonstrated by Lan *et al.* [20] that HHG from molecules with large internuclear distance exhibit strikingly different time-frequency characteristics. The emission times of harmonics with energy beyond $I_p+3.17U_p$ are nearly the same, i.e., well phase locked, and a 95 as isolated attosecond pulse is obtained directly with few-cycle driving pulse. The features discussed above show that the spatially extended systems (molecule with large internuclear distance, atomic clusters, large molecule, etc.) are attractive candidates for generating shorter isolated attosecond pulses directly. However, the critical problems are that the obtained recombination electrons for generating higher-order harmonics are always accompanied by low ionization rate and the bandwidth for isolated attosecond pulse should be further broadened.

In previous work, Bandrauk *et al.* [21] proposed to enhance harmonic generation in extended molecular systems by $\omega+3\omega$ excitation. In this paper, the diatomic molecule with large distance is taken as the research object, for example. The $\omega+3\omega$ and $\omega+2\omega$ schemes are compared; the latter scheme is more appropriate to generate isolated attosecond pulse from stretched molecules with higher efficiency. It is shown that the bandwidth for generating isolated attosecond pulse is significantly broadened to 125 eV and the chirp rate is only 3 as/eV.

II. RESULT AND DISCUSSION

In the present work, we consider the interaction of a diatomic molecule with a linearly polarized intense laser pulse. Though the spatially extended system is complicated, the basic cell is two-body interaction and we take diatomic molecule as the research object to give clear physical pictures.

*Corresponding author; lupeixiang@mail.hust.edu.cn

 ©2009 The American Physical Society

We first give the classical prospect for HHG. The fundamental driving filed, second-harmonic (SH) controlling field and third harmonic (TH) controlling field are linearly polarized along x direction,

$$E_\omega(t) = E_0 \sin\left(\frac{\pi t}{\tau_\omega}\right)^2 \cos(\omega t + \phi_1), \quad (1)$$

$$E_{2\omega}(t) = a_{\omega,2\omega} E_0 \sin\left(\frac{\pi t}{\tau_{2\omega}}\right)^2 \cos(2\omega t + \phi_2 + \phi_{\omega,2\omega}), \quad (2)$$

$$E_{3\omega}(t) = a_{\omega,3\omega} E_0 \sin\left(\frac{\pi t}{\tau_{3\omega}}\right)^2 \cos(3\omega t + \phi_3 + \phi_{\omega,3\omega}), \quad (3)$$

where E_0 is the amplitude and ω is the angular frequency of fundamental driving field. $a_{\omega,2\omega}$ is the ratio of the amplitude between the SH controlling field and the driving field. $a_{\omega,3\omega}$ is the ratio of the amplitude between the TH controlling field and the driving field. τ_ω, $\tau_{2\omega}$, and $\tau_{3\omega}$ are the full width of the pulses. ϕ_1, ϕ_2, and ϕ_3 are the carrier envelope phases of the fields, and $\phi_{\omega,2\omega}$ and $\phi_{\omega,3\omega}$ are the relative phases.

We have considered the amplitude E_0 of the fundamental driving field ($\lambda = 800$ nm) is 0.12 a.u., corresponding to the laser intensity of 5×10^{14} W/cm^2. τ_ω is chosen as $5T_\omega$, where $T_\omega = 2.67$ fs is the oscillation period of the fundamental driving field, and the pulse duration is about 5 fs full width at half maximum. The intensity ratio between SH controlling field ($\lambda = 400$ nm) and driving field is 5% then $a_{\omega,2\omega}$ is 22%. $\tau_{2\omega}$ is set to be $10T_{2\omega}$, where $T_{2\omega} = 1.33$ fs is the oscillation period of the SH controlling field. For the TH controlling field ($\lambda = 267$ nm), $T_{3\omega}$ is 0.89 fs and $a_{\omega,3\omega}$ is also chosen as 22%. The carrier envelope phases ϕ_1, ϕ_2, and ϕ_3 are set to be π, and the relative phases $\phi_{\omega,3\omega}$ and $\phi_{\omega,2\omega}$ are chosen as $-\pi$. It has been demonstrated in Ref. [17] that the electron kinetic energy E_k can reach $8U_p$ when internuclear distance $R = \pi E_0/\omega^2$; thus R is chosen as 115 a.u. In Figs. 1(a), 1(c), and 1(e), the driving field, controlling field, and synthesized electric field are shown as a function of time. By adding the controlling fields to the fundamental driving field, the shape of electric field is changed, leading to ionization ratio modulated between adjacent half cycles. Figures 1(b), 1(d), and 1(f) present the recombined electron kinetic energy as a function of the ionization time calculated by the classical three-step model ($\times$) with the laser fields shown in Figs. 1(a), 1(c), and 1(e), respectively, in the case that electron is ionized from one nucleus and recombines with the neighboring nucleus. If internuclear distance of diatomic molecule is large enough, we can assume that the effect of the neighboring potential can be neglected [22]. None of these treatments above are critical for our conclusions. The tunneling ionization probability is calculated by the atomic Ammosov-Delone-Krainov (ADK) model (gray filled curve) [23]. Obviously, the electrons ionized by the electric field approximating to zero will recombine with the neighboring nucleus with the maximum kinetic energy. Without loss of generality, we take four points [A, B, C, and D in Figs. 1(b), 1(d), and 1(f)] which correspond to the recombined electron kinetic energy about $4.5U_p$, for example, and then the instantaneous ionization probability of these points are analyzed.

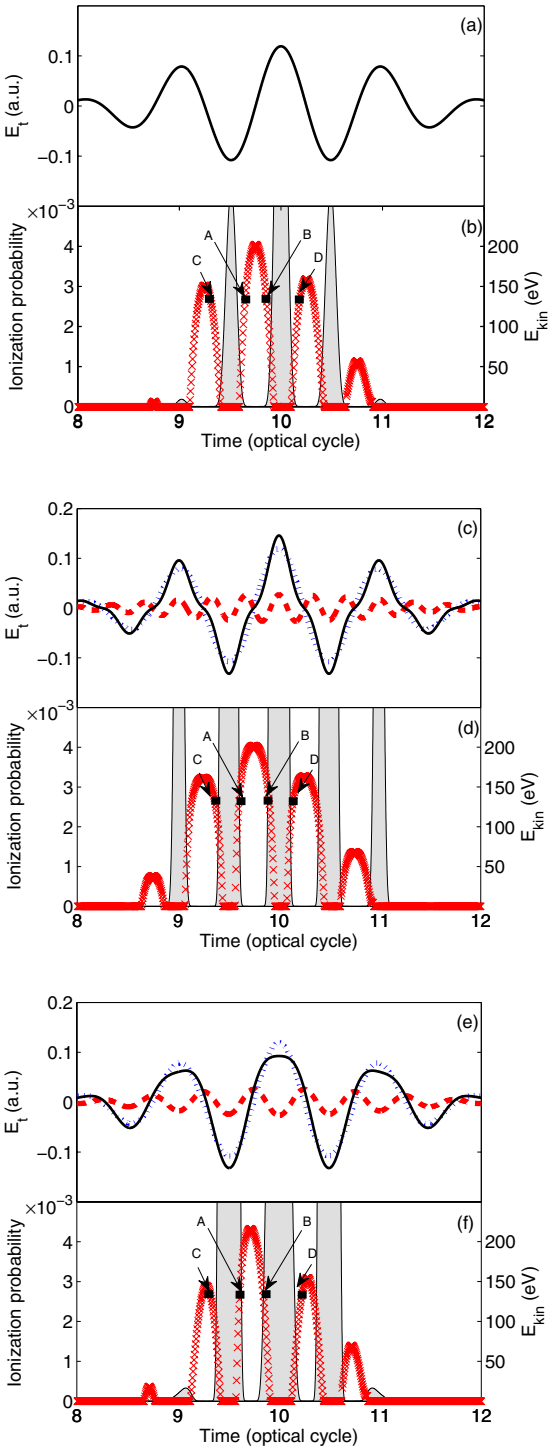

FIG. 1. (Color online) (a) Electric fields of a 5 fs driving laser pulse. (b) Dependence of eletron kinetic energy on the ionization times ($\times$) with driving field shown in (a), in the case that the electron is ionized from one nucleus and recombines with the neighboring nucleus. The gray filled curves show the dependence of ionization probability on time. (c) The synthesized field (solid line) of a 5 fs driving laser pulse (dotted line) in combination with TH controlling field (dashed line). (d) Same as (b) but for the synthesized field shown in (c). (e) The synthesized field (solid line) of a 5 fs driving laser pulse (dotted line) in combination with SH controlling field (dashed line). (f) Same as (b) but for the synthesized field shown in (e).

Obviously, the ionization probability for the points A, B, C, and D in Figs. 1(d) and 1(f) is much higher than those in Fig. 1(b). The results indicate that both $\omega+3\omega$ and $\omega+2\omega$ excitation schemes increase ionization probability of higher-order harmonics. We then focus on the difference of the instantaneous ionization probability between points A, B and C, D. The ionization probability of points A and B are comparable with C and D as shown in Fig. 1(d), whereas points A and B correspond to much higher ionization probability than C and D in Fig. 1(f). This character can be attributed to the shaped electric field by the SH and TH controlling fields. The fundamental driving field is enhanced every half cycle with $\omega+3\omega$ scheme, but $\omega+2\omega$ scheme increases the amplitude in the first half cycle of fundamental driving field and suppresses the amplitude in the next half cycle. The other remarkable feature shown in Fig. 1(f) is that the bandwidth for generating single attosecond pulse reaches 65 eV due to the asymmetric electric field produced by $\omega+2\omega$ scheme. In contrast to Fig. 1(f), the classical calculations in Fig. 1(d) show that the bandwidth for generating single attosecond pulse is limited to 45 eV.

Next, we analyze the response of diatomic molecule by performing *ab initio* simulations of the time-dependent Schrödinger equation (atomic units are used),

$$i\frac{\partial\Psi(x,t)}{\partial t} = [H_0 + E(t)x]\Psi(x,t), \tag{4}$$

where

$$H_0 = -\frac{1}{2}\nabla_x^2 + V(x) \tag{5}$$

is the field-free Hamiltonian. $V(x)$ is Coulomb potential which can be described by

$$V(x) = -\frac{1}{\sqrt{a+(x-R/2)^2}} - \frac{1}{\sqrt{a+(x+R/2)^2}}. \tag{6}$$

Here, the soft core parameter $a=0.5$, R is the internuclear distance, and the two nuclei are fixed at $\pm R/2$. We solve the Schrödinger equation numerically by means of the split operator method [24], starting from the field-free ground state, which is obtained by propagation in imaginary time. It was investigated by Lein [25] that the efficiency of harmonic radiation beyond $I_P+3.17U_p$ from stretched molecule is significantly affected by the initial state. It would achieve a much lower efficiency when the laser-molecule interaction is initialized from the state in which the electron is localized station one center. We have performed each study initially in the gerade state in which the single-electron orbital is coherently delocalized over the two potential wells. Some methods have been proposed to prepare the coherent state of molecules with large internuclear distance. For H_2^+, the coherent state may be realized by using a pump-probe scheme where a moderate-intensity preparation pulse dissociates it before an intense pulse generates high harmonics at the appropriate internuclear separation [25]. The coherent state of more complex molecule such as H_3^+ can be prepared by a cw laser excitation in resonance with the 1σ-3σ transition, and collision of H^+ with $H_2^+(1\sigma_u)$ or from dissociation of the 2σ or 3σ electronic states [26,27]. Then the dipole acceleration $a(t)$ is calculated by Ehrenfest's theorem [28]

$$a(t) = -\langle\Psi(x,t)|\frac{\partial V(x)}{\partial x}|\Psi(x,t)\rangle. \tag{7}$$

The harmonic spectrum is calculated by Fourier transforming the dipole acceleration. To analyze the quantum trajectory, Gabor transform is performed [29]

$$S(\omega,t_c) = \int a(t)W(t-t_c)\exp(-i\omega t)dt, \tag{8}$$

where $W(t-t_c)$ is the temporal window, and t_c represents the center of the window. We choose Kaiser window for the time-frequency analysis, and it can be described by

$$W(t-t_c) = \frac{B_0\left(\beta\sqrt{1-\frac{4(t-t_c)^2}{\tau^2}}\right)}{|B_0(\beta)|}, \tag{9}$$

where B_0 is the modified Bessel function of first kind. τ is the full width of the window in time domain, τ is chosen as 27 a.u. The Kaiser window β parameter that affects the sidelobe attenuation of the Fourier transform of the window, we adopt $\beta=10$.

Figures 2(a), 2(c), and 2(e) show the harmonic radiation from diatomic molecule with large internuclear distance with 5 fs fundamental driving field and two types of synthesized field, respectively. In all of Figs. 2(a), 2(c), and 2(e), the harmonics present a two-plateau structure; the demarcation energy of the two plateaus is $I_p+3.17U_p$. The first plateau is mainly contributed by the electrons ionized from one nucleus and recombine with its parent nucleus, and the second plateau is attributed to the electron ionized from one nucleus and combine with the neighboring nucleus. The ionization time for generating first plateau corresponds to nearly peak of the electric field, while the magnitude of electric field for generate second plateau is lower than the peak value. Thus the first plateau is a few orders of magnitude higher than the second plateau. When the controlling field is added, the instantaneous electric field at ionization time is increased, so the second plateaus both in Figs. 2(c) and 2(e) are about 1 order of magnitude higher than that in Fig. 2(a). Specially, both even and odd harmonics are observed in a wide regime of the second plateau as shown in Fig. 2(e). In Figs. 2(b), 2(d), and 2(f) we present a time-frequency analysis for Figs. 2(a), 2(c), and 2(e). Two and three dominant radiations are visible, respectively, in Figs. 2(b) and 2(d), while only one dominant radiation is remarkable in Fig. 2(f). In Fig. 2(d) the bandwidth for generating single attosecond pulse is 45 eV which is the same as classical prediction shown in Fig. 1(d); however, the bandwidth in Fig. 2(f) is significantly broadened to 125 eV, and the bandwidth is largely increased, comparing with the 65 eV classical result shown in Fig. 1(f). It is because that the influence of ionization probability on harmonic efficiency is included with quantum calculation. The broadened bandwidth gives evidence of ionization modulated by $\omega+2\omega$ excitation scheme. The electron ionization is controlled to induce the change in harmonic efficiency in two successive half cycles: one is enhanced while the other is

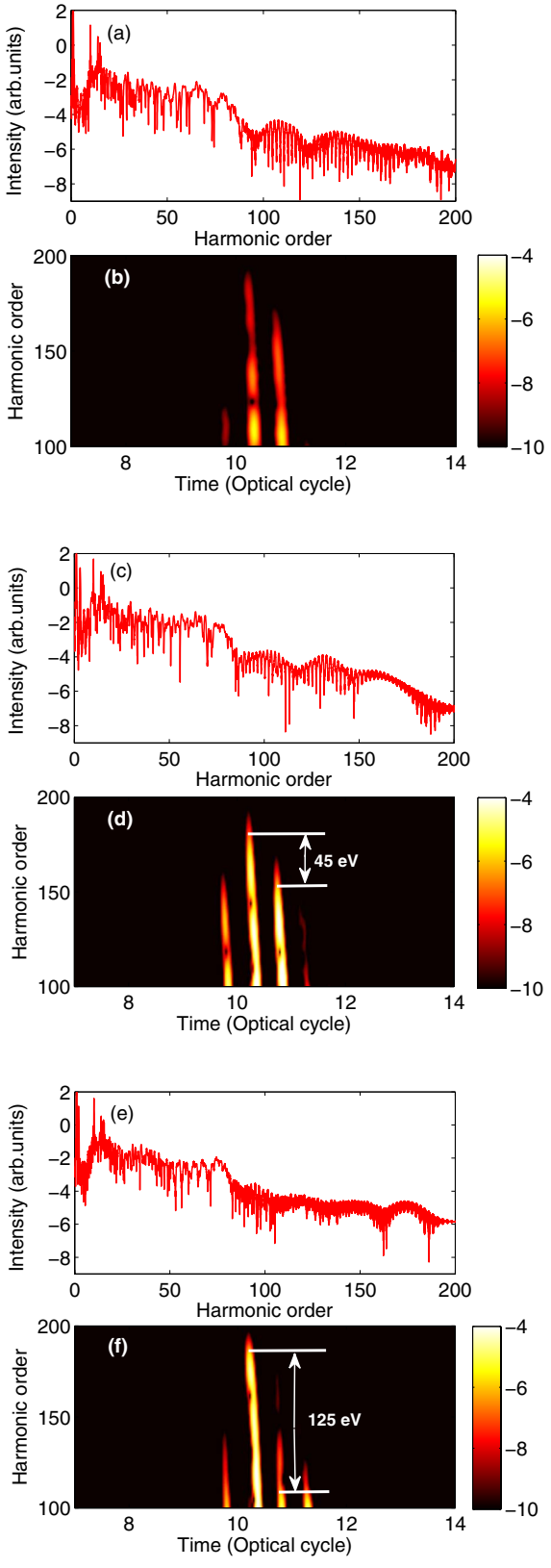

FIG. 2. (Color online) Harmonic spectrum of harmonic radiation from diatomic molecules with large internuclear distance exposed to the (a) 5 fs fundamental field shown in Fig. 1(a) and 1(c) $\omega+3\omega$ synthesized field shown in Fig. 1(c) and 1(e) $\omega+2\omega$ synthesized field shown in Figs. 1(e), 1(b), 1(d), and 1(f) show the time-frequency analysis of (a), (c), and (e), respectively.

suppressed. Thus the results imply that $\omega+2\omega$ excitation scheme is beneficial of generating enhanced broadband single attosecond pulse.

Note that the combined electrons with the same kinetic energy correspond to two different ionization moments [see Figs. 1(b), 1(d), and 1(f)], however, they emission nearly at the same time [see Figs. 2(b), 2(d), and 2(f)]. This imply a better phase-locked property [20]. In addition, we calculated the chirp rate of the radiation with $C=\delta t/\delta E$ [3,30], where t and E are the emission time and energy of harmonics. The calculated chirp rate in our scheme is 3 as/eV approximately, which is much smaller than the typical value of 9 as/eV in atoms [30]. This character can be attributed to more orders of harmonics are radiated in molecules with large internuclear distance, and the duration of radiation time segment is nearly the same as the situation in atoms. The smaller chirp rate allows one to select broader bandwidth for single attosecond generation directly.

Figure 3(a) shows the isolated attosecond pulse generated from harmonic spectrum shown in Fig. 2(b). The available bandwidth is limited to 30 eV, corresponding to 165th–185th-order harmonics. In Fig. 3(b), by selecting the 125th–165th-order harmonics in Fig. 2(b), the temporal profile with two subpulses is presented. The two subpulses can be attributed to the two dominant radiations in Fig. 2(b). We should note that the attosecond radiation in Fig. 3(b) is about 1 order of magnitude higher than that in Fig. 3(a). This can be easily understood by difference of the instantaneous electric field for ionizing between the two cases. The ionization time for generating 165th–185th-order harmonics corresponds to instantaneous electric field near zero, whereas the ionization time for generating 125th–165th-order harmonics correspond to a stronger part of the electric field. As shown in Fig. 1, the ionization time of the relative lower radiated energy corresponds to a stronger part of electric field. Figure 3(c) shows attosecond pulse generation by selecting 105th–145th-order harmonics in Fig. 2(d), three subpulses are presented. Figure 3(d) shows attosecond pulse generation by selecting 105th–145th-order harmonics in Fig. 2(f). It is not only shown a 68 as isolated pulse, which approaches to the 60 as Fourier transform limitation, but also the intensity of the attosecond pulse is further enhanced by about 1 order of magnitude, comparing with the radiation in Fig. 3(b). The higher efficiency can be attributed to two factors: one is the electric field at ionization time is increased with two-color excitation scheme, the other is that harmonic spectrum with relative lower energy is selected for producing isolated attosecond pulse.

Note that all above quantum results are obtained by one-dimensional quantum approach, and one-dimensional model will produce quite reliable results in our scheme due to that the electron predominantly oscillates in the laser polarization direction, which has been used in previous works [21,25,31]. However, one dimension model has some limitations, since the transverse diffusion of electron wave packet is neglected. The three-dimensional expansion of electron wave packet will decrease the efficiency of the harmonic spectrum as shown in [27,31,32]. The electron wave packet generated by tunnel ionization is likely to be quite compact initially, but very rapidly spreads once free of the confining atomic poten-

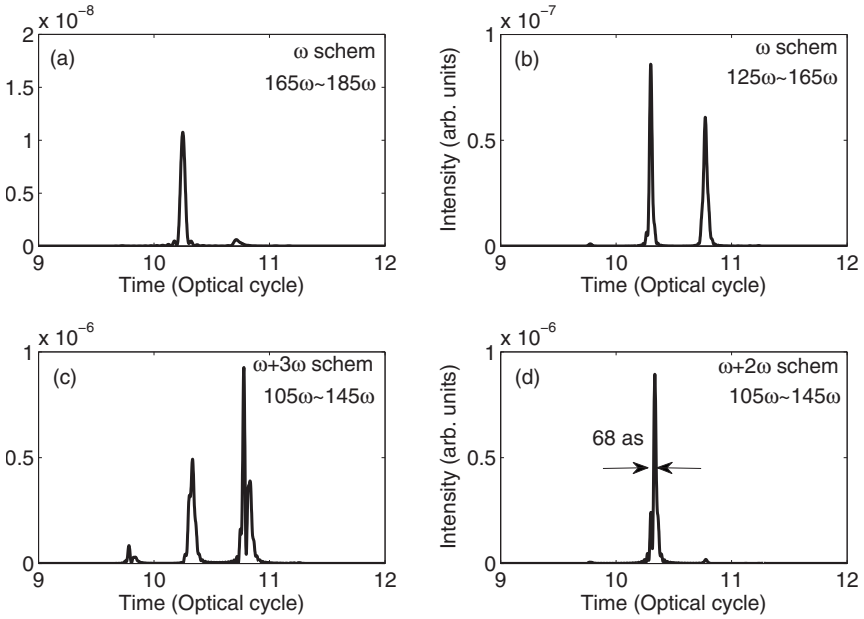

FIG. 3. Temporal profiles of the attosecond pulses generated from harmonic spectrum in Fig. 2. (a) The 165th–185th-order and (b)125th–165th-order harmonics in Fig. 2(b) are selected. (c) The 105th–145th-order harmonics in Fig. 2(d) are selected. (d) The 105th–145th-order harmonics in Fig. 2(f) are selected.

tial. If the initial wave-packet width is $\delta l(0)$ then at time t the width in atomic units is estimated by [33]

$$\delta l(t) = \sqrt{\delta l(0)^2 + [t/2\delta l(0)]^2}, \tag{10}$$

so that the width of the expanded electron wave packet is determined by the traveling time. Our classical calculations show that the traveling times for the electron that recombines with the neighboring nucleus are from 0.4 to 0.8 optical cycles. Including the diffusion of wave packet induced by three-dimensional effect, the transverse widths of the wave packet would be 22–45 a.u. Thus it will achieve a low efficiency including three-dimensional effect.

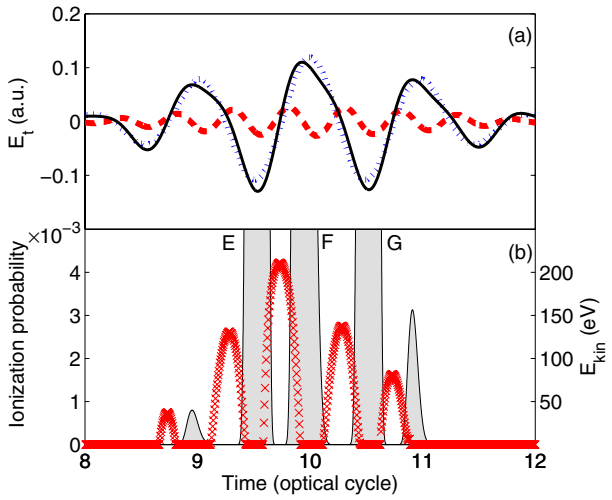

FIG. 4. (Color online) (a) The synthesized field (solid line) of a 5 fs fundamental driving laser pulse (dotted line) in combination with SH controlling field (dashed line), the relative phase between the two fields is -1.25π. (b) Dependence of eletron kinetic energy on the ionization times (×) with driving field shown in (a) and the gray filled curves show the dependence of ionization probability on time.

We then investigate the influence of relative phase between fundamental driving field and SH controlling field on harmonics generation. The electric field is shown in Fig. 4(a), the relative phase $\phi_{\omega,2\omega}$ is chosen as -1.25π; other laser field parameters are the same as those in Fig. 1(e). Figure 4(b) shows the recombined electron kinetic energy E_k as a function of the ionization time (×) in the case that electron is ionized from one nucleus and combines with the neighboring nucleus, and the instantaneous ionization probability is presented by the gray filled curve. The dramatic feature shown in Fig. 4(b) is that the time interval between the two ionization peaks E and F is smaller than that between F and G, whereas the time intervals between the ionization peaks in Fig. 1(e) are almost equal. Thus, the most energetic recombined electrons will correspond to a stronger part of ioniza-

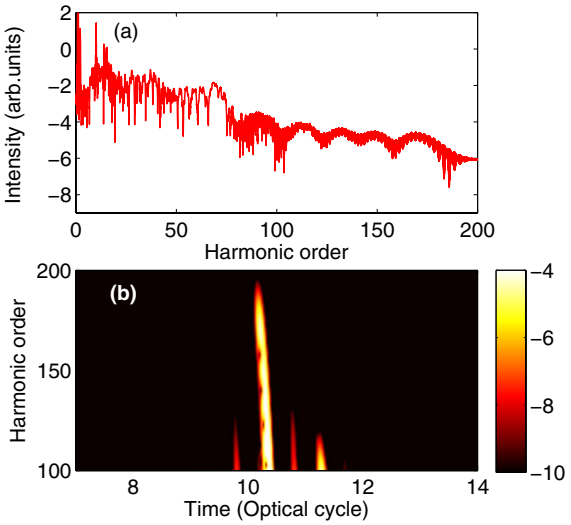

FIG. 5. (Color online) (a) Harmonic spectrum of harmonic radiation from diatomic molecules with large internuclear distance exposed to the $\omega+2\omega$ synthesized field and the relative phase between the two fields is -1.25π.

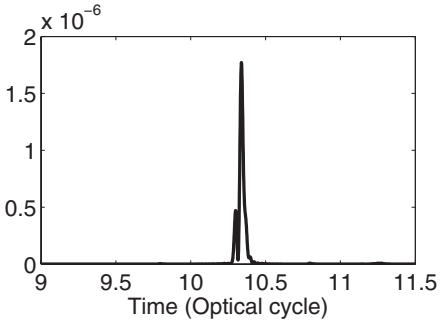

FIG. 6. Temporal profiles of the attosecond pulses generated from harmonic spectrum in Fig. 6. The 105th–145th-order harmonics are selected.

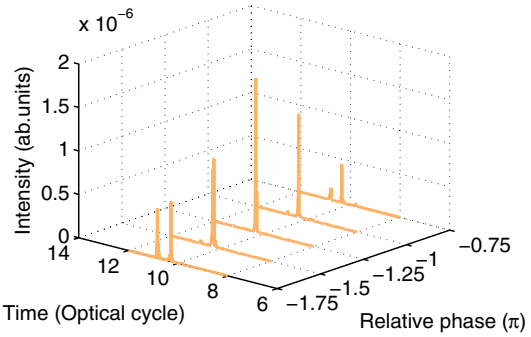

FIG. 7. (Color online) Temporal profiles of the attosecond pulses generated at different relative phase between the fundamental field and SH controlling fields by selecting 105th–145th-order harmonics.

tion peaks when specific relative phase is adopted, and then the efficiency of higher-order harmonics can be further increased. The calculated harmonic spectrum and time-frequency analysis of this spectrum are shown in Figs. 5(a) and 5(b), respectively. Figure 6 shows the temporal profiles of the attosecond pulse by selecting the harmonics from the 105th- to 145th-order harmonics. One can see that the intensity of single attosecond pulse is further increased, comparing with that in Fig. 4(d). In Fig. 7, temporal profiles of the attosecond pulses generated depending on different relative phases between the fundamental field and SH controlling fields by selecting 105th–145th-order harmonics are presented. Our simulation shows that the variation in relative phase $\phi_{\omega,2\omega}$ from -1.5π to $-\pi$ will enable the isolated attosecond pulse production with the side peaks less than 5% of the main peak intensity. The influence of intensity ratio between SH controlling field and fundamental driving field on harmonics generation from stretched molecule is also studied. The variations in intensity ratio from 2–12 % will hardly influence the results in our scheme, except that the intensity of the obtained single attosecond pulse will be further increased with the intensity ratio growth. When the intensity ratio increases to more than 12%, it will achieves a lower phase-locked degree of harmonic radiation beyond $I_p + 3.17U_p$.

III. CONCLUSION

We have studied the generation of high harmonics and isolated attosecond pulse in extended systems with two-color excitation scheme. The diatomic molecule with large distance is taken as the research object for example. The $\omega + 3\omega$ excitation scheme and $\omega + 2\omega$ excitation scheme are compared. It is found that the bandwidth which supports for isolated attosecond pulse is significantly broadened to 125 eV with $\omega + 2\omega$ scheme. The generated 125 eV harmonic is well phase locked and the chirp rate is smaller; these characters benefit of producing a shorter attosecond pulse straightforwardly, for example, an isolated 68 as pulse is obtained in our calculation. Our scheme should be particularly useful in rare-gas clusters [18,19], and for diatomic molecule, such an effect should be observable by dissociating the molecule, letting the nuclei propagate to $R = \pi E_0/\omega^2$ [34]. In addition, the enhanced radiated signal is a useful tool for detecting dynamics processes which occur in the spatially extended system itself.

ACKNOWLEDGMENTS

This work was supported by the National Natural Science Foundation of China under Grants No. 10774054 and No. 10734080 and the National Key Basic Research Special Foundation under Grant No. 2006CB806006.

[1] P. B. Corkum, Phys. Rev. Lett. **71**, 1994 (1993).
[2] P. M. Paul, E. S. Toma, P. Breger, G. Mullot, F. Augè, Ph. Balcou, H. G. Muller, and P. Agostini, Science **292**, 1689 (2001).
[3] Y. Mairesse, A. de Bohan, L. J. Frasinski, H. Merdji, L. C. Dinu, P. Monchicourt, P. Breger, M. Kovačev, R. Taïeb, B. Carreć, H. G. Muller, P. Agostini, and P. Salières, Science **302**, 1540 (2003).
[4] P. Tzallas, D. Charalambidis, N. A. Papadogiannis, K. Witte, and G. D. Tsakiris, Nature (London) **426**, 267 (2003).
[5] M. Hentschel, R. Kienberger, Ch. Spielmann, G. A. Reider, N. Milosevic, T. Brabec, P. Corkum, U. Heinzmann, M. Drescher, and F. Krausz, Nature (London) **414**, 509 (2001).
[6] R. Kienberger, E. Goulielmakis, M. Uiberacker, A. Baltuska, V. Yakovlev, F. Bammer, A. Scrinzi, Th. Westerwalbesloh, U. Kleineberg, U. Heinzmann, M. Drescher, and F. Krausz, Nature (London) **427**, 817 (2004).
[7] G. Sansone, E. Benedetti, F. Calegari, C. Vozzi, L. Avaldi, R. Flammini, L. Poletto, P. Villoresi, C. Altucci, R. Velotta, S. Stagira, S. De Silvestri, and M. Nisoli, Science **314**, 443 (2006).
[8] P. Lan, P. Lu, W. Cao, Y. Li, and X. Wang, Phys. Rev. A **76**, 011402(R) (2007).
[9] W. Cao, P. Lu, P. Lan, X. Wang, and Y. Li, Phys. Rev. A **75**, 063423 (2007).
[10] M. Lein, N. Hay, R. Velotta, J. P. Marangos, and P. L. Knight, Phys. Rev. Lett. **88**, 183903 (2002).
[11] M. Lein, N. Hay, R. Velotta, J. P. Marangos, and P. L. Knight,

Phys. Rev. A **66**, 023805 (2002).
[12] J. Itatani, J. Levesque, D. Zeidler, Hiromichi Niikura, H. Pépin, J. C. Kieffer, P. B. Corkum, and D. M. Villeneuve, Nature (London) **432**, 867 (2004).
[13] T. Kanai, S. Minemoto, and H. Sakai, Nature (London) **435**, 470 (2005).
[14] G. L. Kamta and A. D. Bandrauk, Phys. Rev. A **70**, 011404(R) (2004).
[15] C. C. Chirila and M. Lein, Phys. Rev. A **73**, 023410 (2006).
[16] C. Vozzi, F. Calegari, E. Benedetti, J. P. Caumes, G. Sansone, S. Stagira, M. Nisoli, R. Torres, E. Heesel, N. Kajumba, J. P. Marangos, C. Altucci, and R. Velotta, Phys. Rev. Lett. **95**, 153902 (2005).
[17] P. Moreno, L. Plaja, and L. Roso, Phys. Rev. A **55**, R1593 (1997).
[18] T. D. Donnelly, T. Ditmire, K. Neuman, M. D. Perry, and R. W. Falcone, Phys. Rev. Lett. **76**, 2472 (1996).
[19] C. Vozzi, M. Nisoli, J.-P. Caumes, G. Sansone, S. Stagira, and S. De Silvestri, Appl. Phys. Lett. **86**, 111121 (2005).
[20] P. Lan, P. Lu, W. Cao, X. Wang, and G. Yang, Phys. Rev. A **74**, 063411 (2006).
[21] A. D. Bandrauk, S. Chelkowski, H. Yu, and E. Constant, Phys. Rev. A **56**, R2537 (1997).
[22] P. Moreno, L. Plaja, and L. Roso, J. Opt. Soc. Am. B **13**, 430 (1996).
[23] M. V. Ammosov, N. B. Delone, and V. P. Krainov, Sov. Phys. JETP **64**, 1191 (1986).
[24] M. D. Feit, J. A. Fleck, Jr., and A. Steiger, J. Comput. Phys. **47**, 412 (1982).
[25] M. Lein, Phys. Rev. A **72**, 053816 (2005).
[26] A. D. Bandrauk, S. Barmaki, and G. L. Kamta, Phys. Rev. Lett. **98**, 013001 (2007).
[27] A. D. Bandrauk and S. Barmaki, Chem. Phys. **338**, 312 (2007).
[28] K. Burnett, V. C. Reed, J. Cooper, and P. L. Knight, Phys. Rev. A **45**, 3347 (1992).
[29] P. Lan and P. Lu, Phys. Rev. A **77**, 013405 (2008).
[30] S. Kazamias and Ph. Balcou, Phys. Rev. A **69**, 063416 (2004).
[31] A. D. Bandrauk and H. Yu, Phys. Rev. A **59**, 539 (1999).
[32] A. D. Bandrauk and H. Yu, J. Phys. B **31**, 4243 (1998).
[33] M. Protopapas, C. H. Keitel, and P. L. Knight, Rep. Prog. Phys. **60**, 389 (1997).
[34] H. Stapelfeldt, H. Sakai, E. Constant, and P. B. Corkum, Phys. Rev. A **55**, R3319 (1997).